Performance Comparison of Layered Space Time Codes

Ka Leong Lo, Slavica Marinkovic, Zhuo Chen and Branka Vucetic
The School of Electrical and Information Engineering,
The University of Sydney, NSW 2006, Australia

***Abstract*—Multiple antenna systems have a potential to provide a high capacity in wireless communication systems. The spectral efficiency of space time trellis coding (STTC) is limited by the encoder structure. The layered space time (LST) architecture can overcome this problem. Three different LST schemes are presented. An improved iterative parallel interference canceller (PIC) method is applied at the receiver. A significant performance improvement is achieved compared to the standard PIC. Simulation results of three various layer structures are compared with low density parity check (LDPC) and convolutional codes as component codes.**

I. INTRODUCTION

In [1], Foschini and Gans showed that a high bandwidth efficient communication can be achieved in a wireless fading environment with multi-transmit and receive antennas. Furthermore, the horizontally (HLST) and diagonally (DLST) layered space time structure were proposed to realize this concept [2]. In LST system, the received signal is a superposition of the transmitted coded symbols scaled by the multipath fading coefficients and corrupted by additive white Gaussian noise (AWGN). Interference suppression and interference cancellation techniques are employed in the detector and each constituent code can be decoded individually [2], [3]. In addition, a great performance improvement can be realized by using iterative detection/decoding techniques [4], [5], [6].

Recent simulation results [8], [9] show that performance of LDPC is close to that of turbo codes. The important property of LDPC codes is that the minimum Hamming distance d_{min} of the code increases linearly with the code length [7]. A simple and effective iterative probabilistic decoding algorithm is used to decode this class of codes. The decoding complexity is linearly proportional to the code length. Frame errors are easily detected by the parity check syndrome.

In this paper, the simulation results of the three proposed LST structures are compared. The LST structures with LDPC codes are compared to the respective structures with convolutional codes. The simulation results show that the architectures with LDPC codes outperform those with convolutional codes if there is no interference from other antennas. This can be approached by a system with sufficient number of receive antennas. It shows that the performance of LST is dominated by minimum squared Euclidean distance d_E^2 of the component code when the diversity gain is large. This result is consistent with the conclusion in [10] and [11]. Furthermore, an improved iterative PIC [12] is applied as the detector in LST structures and is shown to achieve the performance of a minimum mean square error (MMSE) iterative receiver, although the complexity of PIC is much lower than that of MMSE.

This project was supported by Norman I Price Fellowship and Nortel Networks.

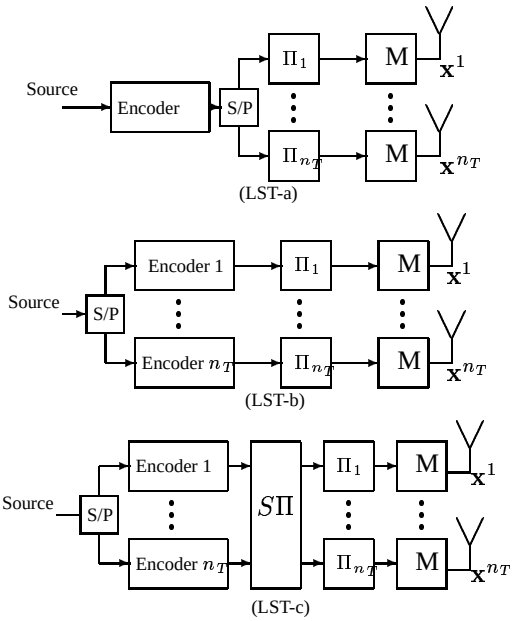

Fig. 1. Layered space time transmit architectures

The remainder of the paper is organized as follows. Section II reviews the system model of LST structures. Section III describes three different proposed LST architectures. Section IV presents the iterative standard PIC, improved PIC and MMSE detections. The improved PIC detector with combining is shown to achieve MMSE performance with similar complexity of standard PIC. Section V presents the simulation results and the conclusion is given in section VI.

0-7803-7400-2/02/$17.00 © 2002 IEEE

II. System model

We consider a wireless system with n_T transmit and n_R receive antennas in a quasi-static flat Rayleigh fading fading channel. We assume that the fading coefficients remain the same over a frame and change independently from one frame to another. The information bits are encoded by the constituent code(s) to generate a matrix **C** of n_T rows. Then each row of **C** is interleaved independently, modulated and transmitted by a separate antenna. The transmitted symbol of antenna i, at time t, is denoted by x_t^i. **H** represents the complex channel matrix with dimension $n_R \times n_T$ and entries, denoted by h_{ji} , represent the fade coefficient from transmit antenna i to receive antenna j. The signal at receive antenna j at time t is given by

$$r_t^j = \sum_{i=1}^{n_T} h_{ji} x_t^i + n_t^j, \quad 1 \le i \le n_T, \;\; 1 \le j \le n_R. \qquad (1)$$

where n_t^j is a statistically independent sample of AWGN with identical variance at each of the receive antenna. The receiver is partitioned into a detector and a decoder for each layer. The iterative decoding principle is applied to pass the probability estimates between the detector and decoders.

III. Layered space time architectures

The transmitters and receivers of three LST structures are shown in Figs. 1 and 2, respectively. In the structure denoted by LST-a [5], a single channel code is employed. After serial to parallel conversion, the n_T encoded bit streams are fed into n_T independent interleavers $(\Pi_1, .., \Pi_{n_T})$. Each interleaved sequence is mapped by a symbol mapper M and transmitted through a permanently assigned antenna. The LST-a receiver shown in Fig. 2 first detects the n_T transmitted streams, de-interleaves each stream and converts n_T parallel streams into one serial stream. A channel decoder operates on the output of the serial to parallel conversion and generates soft decoded sequence. Each of the decoded sequence is interleaved and fed back to the detector.

In the structure denoted by LST-b [2], [3], [4] [5], the information stream is first demultiplexed into n_T parallel sequences, each of which is independently encoded, interleaved, symbol mapped and transmitted through a permanently assigned antenna. At the receiver, the n_T data streams are detected and independently de-interleaved and decoded. This scheme is equivalent to the HLST scheme in [2], [3] and [5].

The structure, denoted by LST-c [4] is obtained from LST-b by introducing a spatial interleaver prior to time interleavers $\Pi_1, .., \Pi_{n_T}$ as shown in Fig . 1. Hence the codeword symbols of each encoder are transmitted over different antennas. Let us consider a system with $n_T = 4$. The operation of $S\Pi$ can be expressed as

$$\begin{pmatrix} c_1^1 & c_2^1 & c_3^1 & c_4^1 & \cdots \\ c_1^2 & c_2^2 & c_3^2 & c_4^2 & \cdots \\ c_1^3 & c_2^3 & c_3^3 & c_4^3 & \cdots \\ c_1^4 & c_2^4 & c_3^4 & c_4^4 & \cdots \end{pmatrix} \cdot \longrightarrow \begin{pmatrix} c_1^1 & c_2^4 & c_3^3 & c_4^2 & \ddots \\ c_1^2 & c_2^1 & c_3^4 & c_4^3 & \ddots \\ c_1^3 & c_2^2 & c_3^1 & c_4^4 & \ddots \\ c_1^4 & c_2^3 & c_3^2 & c_4^1 & \ddots \end{pmatrix} \qquad (2)$$

in which an element of the codeword matrix, denoted by c_t^i, represents the encoded bit of layer i at time t. Similarly, the n_T decoupled data streams are de-interleaved and decoded at the receiver. This structure is similar to the DLST architecture. However, unlike the DLST in [2], [3] and [5], the left bottom of the encoded matrix **C** is not empty and thus this scheme is more spectrally efficient than the DLST.

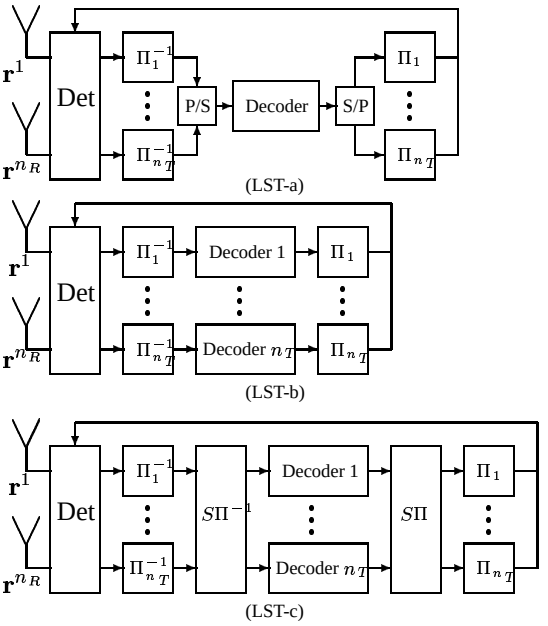

Fig. 2. Layered space time receiver architectures

We assume that the component codes in layers are identical for both LST-b and LST-c structures. In all schemes, the receiver uses an iterative joint detection and decoding. For example, the LST-b detector (Det) shown in Fig. 2 receives sequences, $\mathbf{r}^1, ..., \mathbf{r}^i, ..., \mathbf{r}^{n_R}$, where $\mathbf{r}^i$ is given by $\mathbf{r}^i = (r_1^i, r_2^i, ..., r_l^i)$, representing the received sequence for ith receive antenna, of length l. The decoder estimates the transmitted sequences, $\hat{\mathbf{x}}^1, ..., \hat{\mathbf{x}}^i, ..., \hat{\mathbf{x}}^{n_T}$, where $\hat{\mathbf{x}}^i$ is the estimated sequence transmitted by antenna i. After demodulation and deinterleaving, the transmitted sequence estimates form the input to the channel decoder. The soft output of the decoder is interleaved and fed-back to the detector. In the next iteration, the interference caused by symbols from all other antennas is cancelled by subtracting the soft decoder output on these symbols from the received signal.

IV. Iterative Detection

We consider a standard parallel interference canceller (PIC-STD) [12], [13], its improved version referred as, a parallel interference canceller with decision statistics combining (PIC-CMB) [12] and an MMSE detector [14], [15], [16], as the signal detectors. These detectors are chosen because they offer a good performance-complexity trade-off, particularly when the number of transmit antennas is high and the optimal joint detection and decoding becomes impractical.

In the first iteration, the PIC detectors are equivalent to a bank of matched filters, matched to a vector of channel gains. In the second and later iterations, the estimated mean of the transmitted symbols, from the decoder output is used for interference cancellation.

The PIC-STD detector output in the kth iteration for the symbol transmitted at time t, is arranged in a vector $\hat{\mathbf{x}}_t^k = (\hat{\mathbf{x}}_t^{1,k}, ..., \hat{\mathbf{x}}_t^{n_T,k})^T$ and is given by

$$\hat{\mathbf{x}}_t^k = \mathbf{H}^T \left(\mathbf{r}_t - \mathbf{H}\hat{\mathbf{b}}_t^{k-1} \right), \tag{3}$$

where $\mathbf{r}_t = (r_t^1, ..., r_t^{n_R})^T$ is a $n_R \times 1$ vector of the received signals and $\hat{\mathbf{b}}_t^{k-1} = (\hat{b}_t^{1,k-1}, ..., \hat{b}_t^{n_T,k-1})^T$ is an $n_T \times 1$ vector with symbol estimates as elements except for the ith element which is set to zero. The estimates of the transmitted BPSK symbols are calculated by finding the mean

$$\hat{b}_t^{i,k} = P^k(b_t^i = 1|\hat{\mathbf{x}}^{i,k}) - P^k(b_t^i = -1|\hat{\mathbf{x}}^{i,k}), \tag{4}$$

where $\hat{\mathbf{x}}^{i,k}$ is a vector of detector outputs in the kth iteration for transmit antenna i and $P^k(b_t^i = 1|\hat{\mathbf{x}}^{i,k})$ is the a posteriori probability calculated by the decoder in the kth iteration.

An iterative parallel interference canceller with combining was proposed in [12] for iterative joint detection and decoding to a direct sequence code division multiple access system. The signal at the detector output is modelled as a Gaussian random variable with conditional mean $m_{i,k}$ and variance $\sigma_{i,k}^2$. In a high interference scenario which occurs in a system with a large number of transmit antennas, the detector output in the second iteration becomes significantly biased towards the decision boundary. That is, the conditional mean of the decoder input signal in the second and later iterations is reduced from its nominal value. The other important observation is that for a large number of layers, detector outputs in consecutive iterations are low correlated in early iterations. Under these conditions, a combining method resembling the maximum ratio combining, gives an improved signal-to-noise ratio (SNR).

The optimal weighting coefficients, which maximize SNR after combining, are difficult to estimate or calculate. A practical combining algorithm is obtained by using coefficients which depend only on the variances of the detector outputs in consecutive iterations.

An improved PIC estimate is formed by recursively combining the PIC estimate $\hat{x}_t^{i,k}$ in the current iteration and an improved PIC estimate $(\hat{x}_t^{i,k-1})'$ from the previous iteration

$$(\hat{x}_t^{i,k})' = \frac{(\sigma_{i,k-1}^2)'}{(\sigma_{i,k-1}^2)' + \sigma_{i,k}^2}\hat{x}_t^{i,k} + \frac{\sigma_{i,k}^2}{(\sigma_{i,k-1}^2)' + \sigma_{i,k}^2}(\hat{x}_t^{i,k-1})' \tag{5}$$

where $\sigma_{i,k}^2$ and $(\sigma_{i,k-1}^2)'$ are the variances of the PIC estimate in the kth and improved PIC estimate in the $(k-1)th$ iterations, respectively. The complexity of both PIC-STD and PIC-CMB is linear with the number of transmit antennas.

An iterative MMSE receiver performs parallel interference cancellation and then residual interference suppression [4]. The detector coefficients of an iterative MMSE receiver are derived by minimizing the mean square error between the transmitted signal and a detector output. In the first iteration, transmitted symbols are assumed to be uniformly distributed and hence their a priori probabilities are constant. In later iterations, they are recalculated using the decoder soft outputs in the previous iteration. The updated probabilities are then used to generate the new set of filter coefficients. The MMSE detector output in kth iteration and for the symbol transmitted at time t can be expressed as $\mathbf{y}_t^k = (\mathbf{w}_t^k)^T\hat{\mathbf{x}}_t^k$, where $\hat{\mathbf{x}}_t^k$ is the parallel interference canceller output given by (3) and $\mathbf{w}_t^k$ is the matrix of MMSE filter coefficients. The detector filter coefficients for the transmit antenna i are given by

$$\mathbf{w}_t^{i,k} = \left[\mathbf{H}^T\mathbf{V}_t^i\mathbf{H} + \sigma_n^2\mathbf{I}\right]^{-1}\mathbf{e}^i \tag{6}$$

where $\mathbf{e}^i$ is a column vector of all zeros except the ith element which is 1 and $\mathbf{V}_t^i$ is the covariance matrix between the transmitted and estimated symbols in different layers, given by

$$\begin{aligned}\mathbf{V}_t^i = diag(&1 - (\hat{b}_t^{1,k})^2, 1 - (\hat{b}_t^{2,k})^2, ..., 1 - (\hat{b}_t^{i-1,k})^2, \\ &1, 1 - (\hat{b}_t^{i+1,k})^2, ..., 1 - (\hat{b}_t^{n_T,k})^2).\end{aligned} \tag{7}$$

The direct implementation of the iterative MMSE receiver based on matrix inversion requires a complexity of polynomial order in the number of transmit antennas [4]. However, for quasi-static fading channels, it is possible to implement adaptive MMSE receivers, the complexity of which is linear in the number of transmit antennas.

V. Simulation Results for LST Codes

A. Comparison of LST Structures

In this section, we present simulation results of the three considered LST architectures in a multi-path quasi-static fading channel. A rate 1/2 regular LDPC code with information length 252 and a block-length 504 is chosen as the constituent code. The parity check matrix $\mathbf{H}_{LDPC}$ is constructed as in [7]. Hence, the matrix $\mathbf{H}_{LDPC}$ has a fixed column weight $\gamma = 3$ and a fixed row weight $\rho = 6$. The binary encoded bits are Gray mapped and QPSK modulated prior to transmission, hence there are 252 symbols per frame. PIC-CMB is employed

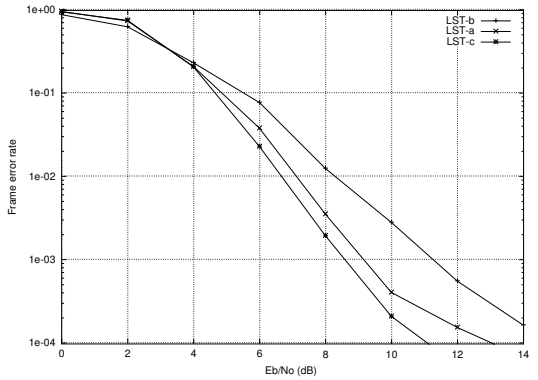

Fig. 3. Performance comparison of three different LST for (n_T, n_R) = (4, 4)

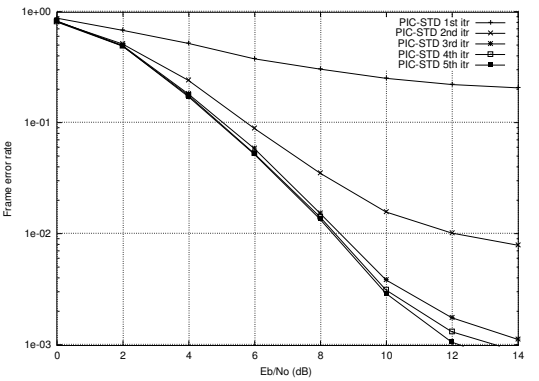

Fig. 4. FER simulation result of LST-b with LDPC and PIC-STD for (n_T, n_R) = (4, 4)

as the detector in the iterative receiver. Five iterations are used between the detector and the decoder. These system parameters are assumed in all simulations unless otherwise stated. The bandwidth efficiency is given by $\eta = \frac{r_b}{B} = n_T R b = n_T$ (b/sec/Hz), where r_b is the data rate, B is the bandwidth, R is the code rate and b is the number of bits per symbol in the signal set.

Fig. 3 shows the frame error rate (FER) performance of the three LST structures with (n_T, n_R) = (4, 4). As shown in Figs. 3 the LST-c has a superior performance compared to LST-a and LST-b. This can be attributed to a higher diversity gain of LST-c than that of the LST-b and its lower sensitivity to the decoder errors than the LST-a. Higher diversity gain is achieved in LST-c because the encoded codeword is transmitted by n_T antennas. Similar to LST-b, received sequences are decoded by n_T channel decoders to provide more reliable feedback in the iteration structure. LST-a obtains a higher diversity gain than LST-b because the encoded sequence is transmitted through different antennas. Therefore, LST-a performs better than LST-b. However, LST-a is more sensitive than LST-b and LST-c to the decoder errors [5]. For example, in LST-b if three of four decoded sequences converge to the correct codewords in the first few iterations, the incorrect layer is likely to converge in later iterations. On the other hand, if a single decoded sequence does not converge in LST-a, the detector will receive an unreliable feedback sequence. The decoder input of the next iteration in this case may not be improved. The error floor of LST-a in Fig. 3 is caused by this effect.

B. Comparison of Different Detection Techniques

In this section, we compare the performance of PIC-STD, PIC-CMB and MMSE for LST-b structure in a system with (n_T, n_R) = (4, 4), BPSK modulation and rate 1/2 LDPC as in the previous section. Fig. 4 shows that a significant error floor is observed with PIC-STD at high E_b/N_o. In Figs. 5 and 6, no error floor is present with either PIC-CMB or MMSE. It can also be observed that MMSE converges slightly faster than PIC-CMB, but both detectors achieve FER of 10^{-3} at less than 12 dB. The main advantage of the proposed PIC-CMB detector is its low complexity compared to MMSE. The complexity of the MMSE detector generally as $O(n_T^3)$, although it can be reduced to $O(n_T^2)$ as shown in [15], while the complexity of both PIC-STD and PIC-CMD are linearly proportional to the number of transmit antennas. In summary, PIC detector with combining has a complexity of standard PIC and achieves the MMSE performance.

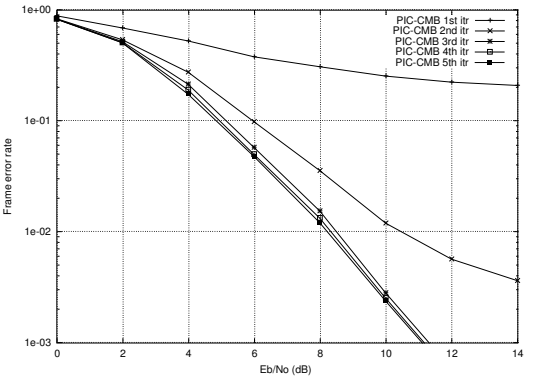

Fig. 5. FER simulation result of LST-b with LDPC and PIC-CMB for (n_T, n_R) = (4, 4)

C. Comparison of LST Structures with Different Constituent Codes

In this section, we compare the performance of three LST structures and decoding complexity of convolutional and LDPC codes. A rate 1/2 convolutional codes with memory order $\nu = 5$ is considered. We use (n, k, ν) to denote a rate k/n convolutional code with memory ν. The generator polynomial in octal form of this code is (53, 75), and the free Hamming distances d_{free} is 8. The d_{min} of the LDPC code ($\gamma = 3$, $\rho = 6$) is calculated as about 11 [7]. The d_{min} and the d_E^2 of these codes are given in Table I. The maximum a posteriori (MAP) and sum-product algorithms are employed to decode convolutional and LDPC codes, respectively. The MAP algorithm

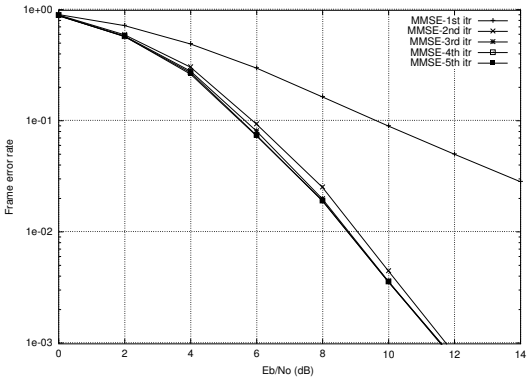

Fig. 6. FER simulation result of LST-b with LDPC and MMSE for (n_T, n_R) = (4, 4)

TABLE I

COMPARISON OF DISTANCE PROPERTY OF CONVOLUTIONAL CODE WITH $\nu = 5$ AND $(\gamma = 3, \rho = 6)$ LDPC CODE WITH CODEWORD LENGTH500

	Conv. $\nu = 5$	LDPC
d_{min}	8	11
d_E^2	16	22

[17] is an optimal trellis based decoding method which minimizes the symbol error probability. A MAP algorithm is used in iterative detection and decoding process. An LDPC code is represented by a factor graph or a belief network [7], [18], [8]. The sum-product algorithm is a probabilistic suboptimal method for decoding graph based codes. This is a syndrome decoding method which finds the most probable vector to satisfy all syndrome constraints. Although the soft-output of this decoder is not the true a posteriori probability because the factor graph of an LDPC code has many cycles, a good error correcting performance is achieved [19]. Furthermore, the probabilistic soft-input of the sum-product algorithm is calculated based on the channel model, CSI and the noise variance. Hence, the decoding algorithm is sensitive to channel estimation errors.

The decoding complexity of MAP algorithm increases exponentially with the memory order ν. On the other hand, the complexity of decoding LDPC code is linearly proportional to the number of entries in the parity check matrix $\mathbf{H}_{LDPC}$. Table II shows the complexity of the two decoding algorithms [17]. It shows the numbers of operations in a single decoding process. The total numbers of operations for an information bit in the MAP decoder are listed in column one. The sum-product decoder is an iterative algorithm, so column two shows the numbers of operations for an information bit in each sum-product iteration. Table II shows that LDPC decoder applies exponential operations to initialize the probabilities of the input sequence while the number of exponential operations of the MAP decoder is proportional to 2^ν. In the simulations, we observe that in most cases, an LDPC code converges within 10

TABLE II

COMPLEXITY OF MAP AND SUM-PRODUCT ALGORITHM

	MAP (per info. bit)	Sum-Product (per info. bit in each iteration)
add.	$2 \cdot 2 \cdot 2^\nu + 6$	$\frac{3 \cdot \gamma}{(1-\gamma/\rho)}$
multpl.	$5 \cdot 2 \cdot 2^\nu + 8$	$\frac{\gamma \cdot (2\gamma+\rho+2)}{(1-\gamma/\rho)}$
exp.	$2 \cdot 2 \cdot 2^\nu + 8$	$\frac{1}{1-\gamma/\rho}$ (initialization)

iterations. The numbers of decoding operations of the codes with codeword length 500 are listed in Table III, along which the results of sum-product algorithm, calculated on the basis of 10 iterations. Fig. 7 shows the performance of three LST

TABLE III

COMPLEXITY COMPARISON BETWEEN CONVOLUTIONAL CODE WITH $\nu = 5$ AND $(\gamma = 3, \rho = 6)$ LDPC CODE WITH CODEWORD LENGTH500

	MAP $\nu = 5$	Sum-Product
add.	33500	45000
multpl.	82000	210000
exp.	32000	500

structures with (n_T, n_R) = (4, 4) and (2, 1, 5) convolutional code. It is shown that LST-c outperforms LST-b considerably and LST-a slightly. We compare the performance of LDPC and

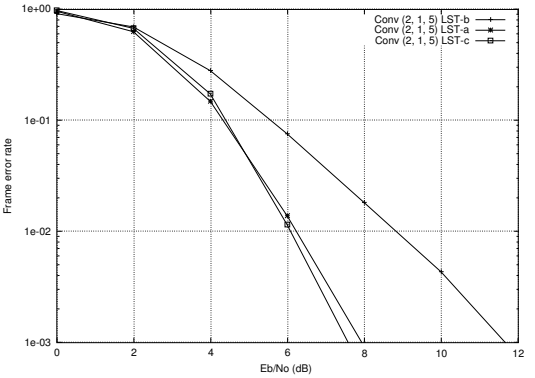

Fig. 7. Performance comparison of three different LST structures with the (2,1,5) convolutional code as a constituent code for (n_T, n_R) = (4, 4)

convolutional codes. Table IV shows the required E_b/N_o for FER of 10^{-3} in three LST structures with (n_T, n_R) = (4, 4). In LST-b, the LDPC outperforms the convolutional code but has a worse performance compared to (2, 1, 5) convolutional code in both LST-a and LST-c structures. Although the LDPC code has a higher distance than the convolutional codes, it has a worse performance. In addition, we notice in Fig. 3 that there exist error floors for the LDPC code in LST structures with $n_R = 4$. However no error floor occurs for convolutional code in Fig. 7. The reason for that is that the sum-product algorithm is more sensitive to decoding errors than the MAP decoder used for

convolutional codes. As mentioned before, it is a probabilistic suboptimal algorithm and it is very sensitive to the estimation decoder errors.

TABLE IV

PERFORMANCE COMPARISON BETWEEN CONVOLUTIONAL CODE WITH $\nu = 5$ AND LDPC CODE IN LST STRUCTURES FOR (n_T, n_R) = (4, 4)

	Conv. $\nu = 5$	LDPC
LST-a	8.0	9.2
LST-b	11.6	11.0
LST-c	7.6	8.8
LST-c (perfect decoding feedback)	8.2	4.9

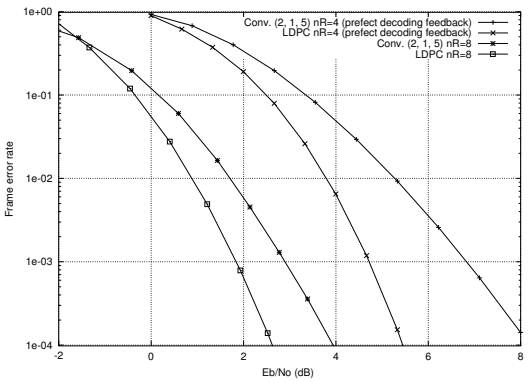

Fig. 8. Performance comparison of LST-c with convolutional and LDPC codes for (n_T, n_R) = (4, 4) with perfect decoding feedback and (n_T, n_R) = (4, 8)

Fig. 8 shows the performance of the two codes in LST-c with no interference. The LDPC code outperforms the convolutional code significantly because the d_E^2 and d_{min} of the LDPC code are larger than those of the convolutional code. The last row of Table IV shows the required E_b/N_o (in dB) of both codes achieving FER of 10^{-3} in the (4, 4) LST-c system with perfect decoding feedback. It shows that the performance difference between perfect and non-perfect decoding feedback of convolutional and LDPC codes are about 0.4 and 3.9 dB, respectively. This means that the iterative joint detection and MAP decoding algorithm approaches no interference performance. As the number of receive antennas increases, the detector can provide better estimates of the transmitted symbols to the channel decoder. In this situation, the distance of the code dominates the LST system performance. Fig. 8 shows that the LDPC code outperforms this convolutional code in a (4, 8) LST-c system. We conclude that the LDPC code has a superior error correction capability, but the performance is limited by feedback decoding errors in LST-a and LST-c structures.

VI. CONCLUSION

We have compared and shown the simulation results of three different LST structures. LDPC and convolutional codes are used as constituent codes. The LST-c is shown to achieve the best performance because it has a high diversity gain and low sensitivity to the decoder errors. Furthermore, we have shown that the PIC detector with decision statistics combining has a complexity of the standard PIC. We conclude that it achieves the MMSE performance with much lower complexity. The decoding complexity and performance comparisons of LDPC and convolutional codes are also given. LDPC codes with good distance properties and low decoding complexity outperform convolutional codes, but the performance is limited by the feedback decoding errors.

REFERENCES

[1] G. Foschini and M. J. Gans, "On limits of wireless communications in a fading environment when using multiple antennas," *Wireless Personal Communications*, vol. 6, pp. 311–355, Mar. 1998.

[2] G. Foschini, "Layered space-time architecture for wireless communication in a fading environment when using multi-element antennas," *Bell Labs Technical Journal*, vol. 1, no. 2, pp. 41–59, 1996.

[3] D. Shiu and J. Kahn, "Layered space-time codes for wireless communications using multiple transmit antennas," *Proc. of IEEE International Conference on Communication, Vancouver, B.C.*, Jun. 1999.

[4] H. E. Gamal and J. A. R. Hammons, "The layered space-time architecture: A new perspective," Submitted to IEEE Transactions on Information Theory.

[5] S. L. Ariyavisitakul, "Turbo space-time processing to improve wireless channel capacity," *IEEE Trans. Commun.*, vol. 48, pp. 1347–1358, Aug. 2000.

[6] D. Shiu and J. Kahn, "Scalable layered space-time codes for wireless communications: Performance analysis and design criteria," *Proc. of IEEE Wireless Communication and Networking Conference, New Orleans, LA*, Sep. 1999.

[7] R. G. Gallager, *Low density parity check codes.* M.I.T., 1963.

[8] D. J. C. MacKay, "Good error–correcting codes based on very sparse matrices," in *Proc. of 1997 IEEE International Symposium on Information Theory. Ulm, Germany.*, p. 113, 1997.

[9] S. Chung, D. Forney, T. Richardson, and R. Urbanke, "On the design of low-density parity-check codes within 0.0045 db of the shannon limit," *IEEE Commun. Lett.*, vol. 5, pp. 58–60, Feb. 2001.

[10] J. Yuan, Z. Chen, B. Vucetic, and W. Firmanto, "Performance analysis and design of space-time coding on fading channels," submitted to IEEE Trans. Commun.

[11] Z. Chen, B. Vucetic, J. Yuan, and K. Lo, "Space-time trellis codes for 4-PSK with three and four transmit antennas in quasi-static flat fading channels," to appear in IEEE Comm. Lett., Feb. 2002.

[12] S. Marinkovic, B. Vucetic, N. Ishii, S. Yoshida, and A. Ushirokawa, "Space-time iterative and multistage receiver structures for cdma mobile communication systems," *IEEE J. on Select Areas in Commun.*, vol. 19, pp. 1594–1604, Aug. 2001.

[13] J. G. Proakis, *Digital Communications.* Mcgraw-hill International, 3 ed., 1995.

[14] X. Wang and H. V. Poor, "Iterative (turbo) soft interference cancellation and decoding for coded cdma," *IEEE Trans. Commun.*, vol. 47, pp. 1046–1061, Jul. 1999.

[15] M. Moher, "An iterative multiuser decoder for near-capacity communiocations," *IEEE Trans. Commun.*, vol. 46, pp. 870–880, Jul. 1998.

[16] H. E. Gamal and E. Geraniotis, "Iterative multiuser detection for coded CDMA in AWGN and fading channels," *IEEE J. on Select Areas in Commun.*, vol. 18, pp. 30–41, Jan. 2000.

[17] B. Vucetic and J. Yuan, *Turbo codes principles and applications.* Kluwer Academic Publishers, 2000.

[18] F. R. Kschischang, B. J. Frey, and H. Loeliger, "Factor graphs and the sum-product algorithm," *IEEE Trans. Infor. Theory*, vol. 47, pp. 498–519, Feb. 2001. http://www.cs.utoronto.ca/ frank/factor/.

[19] D. J. C. MacKay and R. M. Neal, "Near Shannon limit performance of low density parity check codes," *Electronics Letters*, vol. 32, pp. 1645–1646, Aug. 1996. Reprinted *Electronics Letters*, vol 33, no 6, 13th March 1997, p.457–458.